



# Stringent Expression Control of Pathogenic R-body Production in Legume Symbiont *Azorhizobium caulinodans*

Jun-ichi Matsuoka,<sup>a</sup> Fumiko Ishizuna,<sup>b</sup> Keigo Kurumisawa,<sup>c</sup> Kengo Morohashi,<sup>c</sup> Tetsuhiro Ogawa,<sup>b</sup> Makoto Hidaka,<sup>b</sup> Katsuharu Saito,<sup>d</sup> Tatsuhiro Ezawa,<sup>e</sup>  Toshihiro Aono<sup>a</sup>

Biotechnology Research Center, The University of Tokyo, Tokyo, Japan<sup>a</sup>; Graduate School of Agricultural and Life Sciences, The University of Tokyo, Tokyo, Japan<sup>b</sup>; Faculty of Science and Technology, Tokyo University of Science, Tokyo, Japan<sup>c</sup>; Faculty of Agriculture, Shinshu University, Matsumoto, Nagano, Japan<sup>d</sup>; Graduate School of Agriculture, Hokkaido University, Sapporo, Hokkaido Prefecture, Japan<sup>e</sup>

**ABSTRACT** R bodies are insoluble large polymers consisting of small proteins encoded by *reb* genes and are coiled into cylindrical structures in bacterial cells. They were first discovered in *Caedibacter* species, which are obligate endosymbionts of paramecia. *Caedibacter* confers a killer trait on the host paramecia. R-body-producing symbionts are released from their host paramecia and kill symbiont-free paramecia after ingestion. The roles of R bodies have not been explained in bacteria other than *Caedibacter*. *Azorhizobium caulinodans* ORS571, a microsymbiont of the legume *Sesbania rostrata*, carries a *reb* operon containing four *reb* genes that are regulated by the repressor PraR. Herein, deletion of the *praR* gene resulted in R-body formation and death of host plant cells. The *rebR* gene in the *reb* operon encodes an activator. Three PraR binding sites and a RebR binding site are present in the promoter region of the *reb* operon. Expression analyses using strains with mutations within the PraR binding site and/or the RebR binding site revealed that PraR and RebR directly control the expression of the *reb* operon and that PraR dominantly represses *reb* expression. Furthermore, we found that the *reb* operon is highly expressed at low temperatures and that 2-oxoglutarate induces the expression of the *reb* operon by inhibiting PraR binding to the *reb* promoter. We conclude that R bodies are toxic not only in paramecium symbiosis but also in relationships between other bacteria and eukaryotic cells and that R-body formation is controlled by environmental factors.

**IMPORTANCE** *Caedibacter* species, which are obligate endosymbiotic bacteria of paramecia, produce R bodies, and R-body-producing endosymbionts that are released from their hosts are pathogenic to symbiont-free paramecia. Besides *Caedibacter* species, R bodies have also been observed in a few free-living bacteria, but the significance of R-body production in these bacteria is still unknown. Recent advances in genome sequencing technologies revealed that many Gram-negative bacteria possess *reb* genes encoding R-body components, and interestingly, many of them are animal and plant pathogens. *Azorhizobium caulinodans*, a microsymbiont of the tropical legume *Sesbania rostrata*, also possesses *reb* genes. In this study, we demonstrate that *A. caulinodans* has ability to kill the host plant cells by producing R bodies, suggesting that pathogenicity conferred by an R body might be universal in bacteria possessing *reb* genes. Furthermore, we provide the first insight into the molecular mechanism underlying the expression of R-body production in response to environmental factors, such as temperature and 2-oxoglutarate.

**KEYWORDS** R body, legume, pathogenesis, *reb* gene, rhizobia, symbiosis

Received 29 April 2017 Accepted 21 June 2017 Published 25 July 2017

**Citation** Matsuoka J-I, Ishizuna F, Kurumisawa K, Morohashi K, Ogawa T, Hidaka M, Saito K, Ezawa T, Aono T. 2017. Stringent expression control of pathogenic R-body production in legume symbiont *Azorhizobium caulinodans*. *mBio* 8:e00715-17. <https://doi.org/10.1128/mBio.00715-17>.

**Editor** Steven E. Lindow, University of California, Berkeley

**Copyright** © 2017 Matsuoka et al. This is an open-access article distributed under the terms of the [Creative Commons Attribution 4.0 International license](https://creativecommons.org/licenses/by/4.0/).

Address correspondence to Toshihiro Aono, [uaono@mail.ecc.u-tokyo.ac.jp](mailto:uaono@mail.ecc.u-tokyo.ac.jp).

J.M. and F.I. contributed equally to this article.

**R**bodies are bacterial inclusion bodies and are large proteinaceous ribbons that are coiled into cylindrical structures. R bodies were first observed in *Caedibacter* species, which are obligate endosymbiotic bacteria that inhabit paramecia (1). Paramecia that harbor R-body-producing *Caedibacter* cells are referred to as killer paramecia and release bacterial cells via the cytophyge. Subsequently, sensitive nonendosymbiotic paramecia are killed following ingestion of the released bacteria (2), conferring the “killer trait” of paramecia (3). R bodies play a major role in this trait, because paramecia harboring mutant *Caedibacter* strains that are defective in R body production do not express the killer trait (4).

The genes involved in R-body production were originally identified in *Caedibacter taeniospiralis* (5) and include *rebA*, *rebB*, *rebC*, and *rebD* (5, 6). Moreover, genes that are homologous to *rebA*, *rebB*, and *rebD* of *C. taeniospiralis* have been found in species of the phylum *Proteobacteria* and in *Kordia algicida* OT-1 (7), which belongs to the phylum *Bacteroidetes*, whereas no *rebC*-homologous genes have been identified in bacteria other than *C. taeniospiralis* (8, 9). It is hypothesized that *reb*-homologous genes were passed on by horizontal gene transfer—i.e., by phages or plasmids (2, 8, 10, 11). Although many bacterial species that carry *reb*-homologous genes are pathogenic to plants and animals (e.g., *Xanthomonas axonopodis* pv. *citri*, *Stenotrophomonas maltophilia*, *Burkholderia pseudomallei*, and so on) (8), the rhizobium *Azorhizobium caulinodans* ORS571, a mutualistic microsymbiont of the tropical legume *Sesbania rostrata*, possesses *reb*-homologous genes (8, 12). To date, *reb*-homologous genes have not been found in rhizobia other than *A. caulinodans* ORS571.

*A. caulinodans* ORS571 fixes atmospheric nitrogen in free-living and symbiotic states (13–15) and forms nitrogen-fixing nodules at the sites of adventitious root primordia on roots and stems. Bacteria enter stems via fissures at root primordia and colonize cortical infection pockets (16). From these infection pockets, infection threads guide the bacteria toward the nodule meristematic zone, where they are released into host cells and surrounded by plant-derived peribacteroid membranes (16). Subsequently, infected host cells are filled with differentiated bacteroids and infected areas enlarge with nodule maturation (15, 16).

The *A. caulinodans* ORS571 strain has a gene cluster containing four *reb*-homologous genes (8, 12) that are strongly suppressed by *PraR*, which is a conserved transcription factor among *Alphaproteobacteria* (8). In a previous study, stem nodules harboring *A. caulinodans praR* mutants that expressed high levels of *reb* genes were defective in nitrogen fixation (8). Furthermore, *praR* knockout in these nodules altered the interactions between these bacteria and their host cells according to two distinctly abnormal patterns. Specifically, host cells maintained normal shapes, and the bacteria disappeared with increasing host vacuolar sizes, or bacteria predominantly occupied host cells that had shrunken gradually (8). These observations suggest that derepression of *reb* genes at least partially reverts pathogenic traits for the symbiont. The regulatory mechanism underlying the expression of *reb* genes, however, is yet to be elucidated.

In *Caedibacter* spp., *reb* genes are responsible for the production of R bodies, which likely mediate eukaryotic cell death (4, 5). Although *reb* genes have been identified in many pathogenic bacteria, pathogenic roles of R bodies have not been directly demonstrated. On the other hand, observations of disordered intracellular symbiosis in plant hosts following derepression of *reb* genes in *A. caulinodans* suggest that *A. caulinodans* kills host cells by producing R bodies. Herein, we investigated the regulatory mechanism of *reb* gene expression in *A. caulinodans* and defined the roles of R bodies in *reb*-associated pathogenic traits, with particular emphasis on transcription repressor-activator interactions.

## RESULTS

**Genetic organization of the *reb* operon.** The *reb* operon includes genes from AZC\_3781 to AZC\_3788 on the genome of *A. caulinodans* ORS571 (Fig. 1), and transcription units and start sites were determined using reverse transcription-PCR (RT-PCR) and primer extension analyses (see Fig. S1 in the supplemental material). A compre-

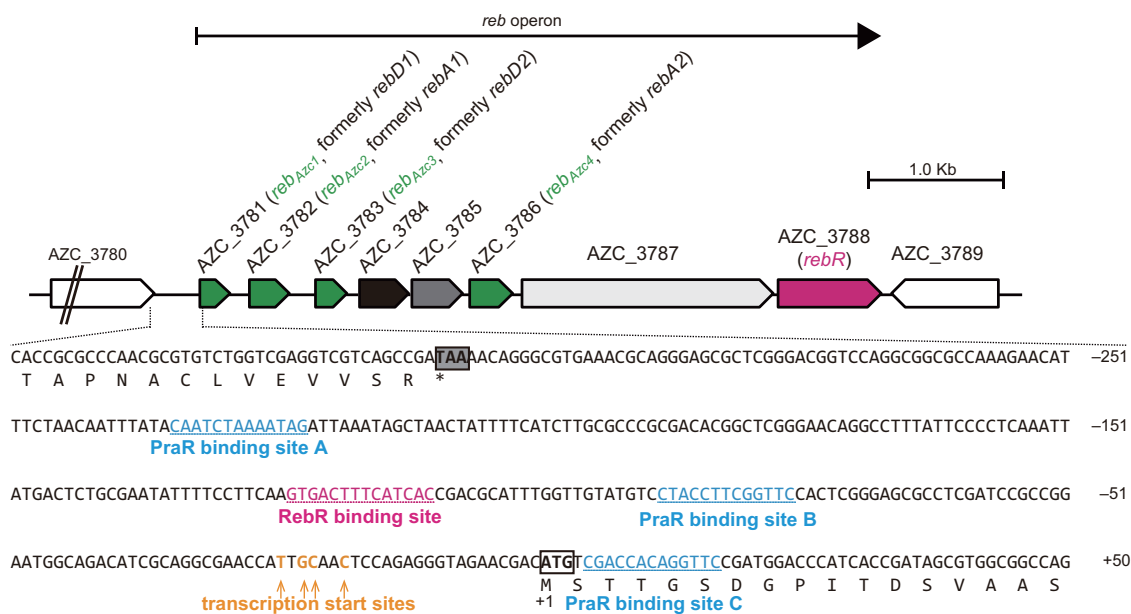


**FIG 1** Genetic organization of the *reb* operon on the chromosome of *A. caulinodans* ORS571. The nucleotide sequence below the map shows the promoter region of the *reb* operon. Deduced amino acid sequences of the C terminus of the AZC\_3780 protein and the N terminus of the Reb<sub>AZC1</sub> protein are shown under their corresponding nucleotide sequences, respectively. The stop codon of AZC\_3780 and the start codon of *reb*<sub>AZC1</sub> are marked by gray and open boxes, respectively. The three PraR binding sites and the RebR binding site are underlined. Transcription start sites of the *reb* operon are indicated by arrows.

hensive phylogenetic analysis revealed that the proteins encoded by *reb* genes in *A. caulinodans* did not belong to clusters, including RebA, RebB, and RebD of *C. taeniospiralis* (see Fig. S2 in the supplemental material). Accordingly, the *reb*-homologous genes (AZC\_3781, AZC\_3782, AZC\_3783, and AZC\_3786) *rebD1*, *rebA1*, *rebD2*, and *rebA2* (8) were renamed *reb*<sub>AZC1</sub>, *reb*<sub>AZC2</sub>, *reb*<sub>AZC3</sub>, and *reb*<sub>AZC4</sub>, respectively. An InterProScan analysis revealed that the AZC\_3788 gene, which was designated *rebR*, encoded a putative transcription factor of the cyclic AMP receptor protein-fumarate and nitrate reduction regulator (Crp-Fnr) superfamily (17). The AZC\_3784, AZC\_3785, and AZC\_3787 genes had no similarities to known *reb* genes, although BLASTp searches identified AZC\_3784 homologues in *Rhizobium* sp. strain AAP43, *Oceanicaulis* sp. strain HTCC2633, and *Oceanicaulis alexandrii* DSM 11625, as well as an AZC\_3787 homologue in *Inquilineus limosus*. However, no AZC\_3785 homologues were found in the database.

**Contributions of the *reb* operon to R-body formation.** To identify roles of the *reb* operon in R-body formation, we generated a *praR* deletion ( $\Delta praR$ ) mutant, a deletion mutant with deletion of a region from AZC\_3781 to AZC\_3787 ( $\Delta AZC_3781-7$ ), and a  $\Delta praR \Delta AZC_3781-7$  double mutant and observed phenotypes of stem nodules at 14 days postinoculation (dpi) with these mutant and wild-type (WT) bacteria. The nitrogen-fixation-defective (Fix<sup>-</sup>) phenotype of the stem nodules carrying bacteria with the *praR* deletion was suppressed by the second deletion in the AZC\_3781-7 region (Fig. 2A), as observed previously (8), whereas the AZC\_3781-7 deletion did not affect *reb* operon expression levels (Fig. 2B). Transmission electron microscopy (TEM) observations showed that R bodies were produced in many  $\Delta praR$  bacterial cells in shrunken host cells, and many R-body-containing bacterial cells had collapsed appearances (Fig. 2C). R bodies were not observed in stem nodules harboring the double mutant (Fig. 2C), suggesting that genes that are essential for R-body formation are located in the region from AZC\_3781 to AZC\_3787.

To observe the dynamics of host-bacterium interactions in single nodules harboring the  $\Delta praR$  mutant, pathogenic roles of R bodies were observed at an early stage of nodule development (7 dpi). Some normal-shape host cells contained bacterial cells that lacked R bodies (Fig. 3A and B), and nuclei in these normal-shape host cells were intact (Fig. 3C). In contrast, R bodies were observed in bacteria within shrunken host

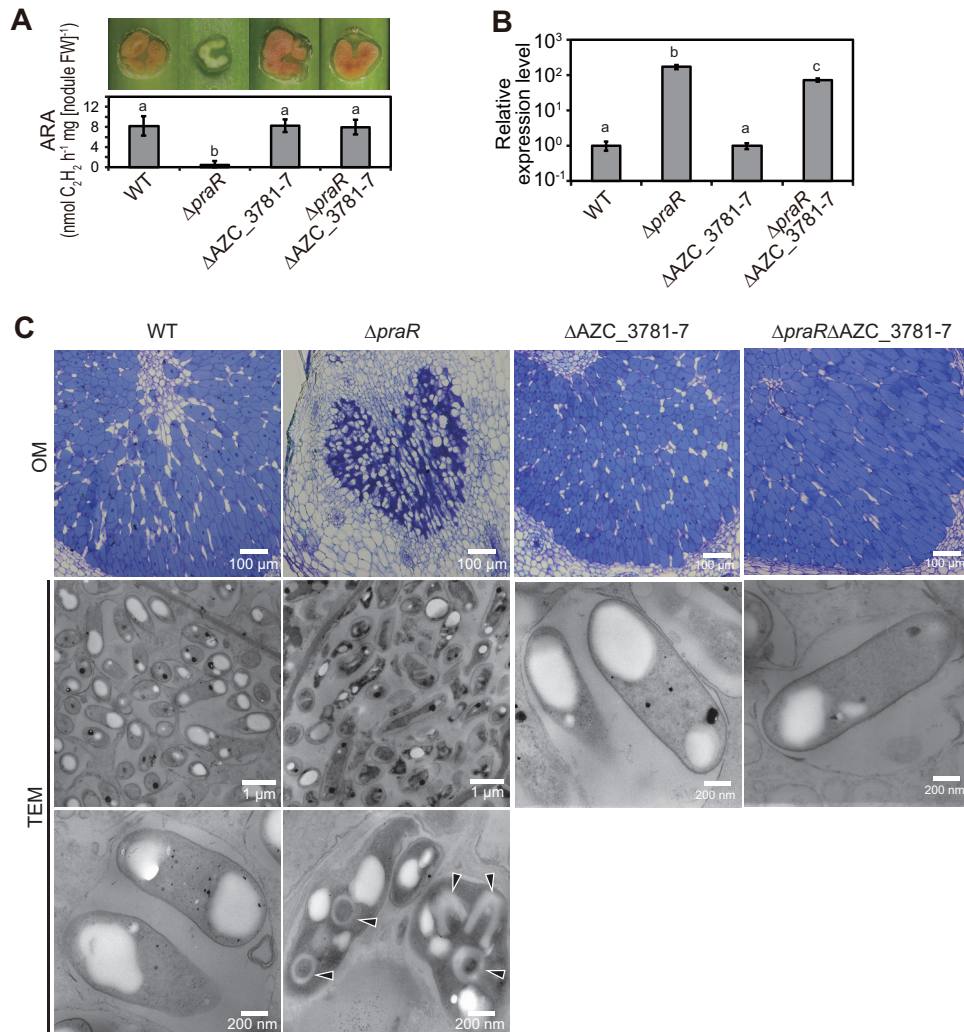


**FIG 2** Contributions of the *reb* operon to R-body formation in stem nodules. *S. rostrata* plants were inoculated with the WT or  $\Delta praR$ ,  $\Delta AZC_{3781-7}$ , or  $\Delta praR \Delta AZC_{3781-7}$  mutant strains and grown at 30°C. Stem nodules were analyzed at 14 days postinoculation (dpi). (A) Hand-cut images (upper) and acetylene reduction activities (ARAs) reflecting nitrogen-fixing activities (lower) of stem nodules. Values are presented as means  $\pm$  standard deviations from five separate plants. Different letters indicate significant differences ( $P < 0.05$ , Tukey-Kramer). (B) Quantitative reverse transcription-PCR (RT-PCR) analyses of the *reb* operon in stem nodules. Expression levels of the *reb* operon were normalized to 16S rRNA levels, expressed relative to corresponding data from the WT strain, and are presented as means  $\pm$  standard deviations from three separate plants. Different letters indicate significant differences ( $P < 0.05$ , Tukey-Kramer). (C) Optical microscopic (OM) observations of infected host cells in stem nodules and transmission electron microscopic (TEM) observations of bacterial cells in host cells. Arrowheads indicate R bodies.

cells (Fig. 3A and D), in which nuclei were collapsed (Fig. 3E), indicating that R-body production is associated with host cell death in the nodules.

Requirements of the non-*reb*-homologous genes *AZC\_3784*, *AZC\_3785*, and *AZC\_3787* and the *reb*-homologous genes *reb<sub>AZC1</sub>*, *reb<sub>AZC2</sub>*, *reb<sub>AZC3</sub>*, and *reb<sub>AZC4</sub>* for R-body production were determined in  $\Delta praR$  mutant derivatives with the deletions of these genes. In these experiments, *AZC\_3784* was essential for R-body formation and *AZC\_3785* and *AZC\_3787* were not (see Fig. S3 in the supplemental material). In addition, both *reb<sub>AZC3</sub>* and *reb<sub>AZC4</sub>* and either *reb<sub>AZC1</sub>* or *reb<sub>AZC2</sub>* were essential for R-body production (see Fig. S4 in the supplemental material).

In investigations of the contributions of RebR to nodule formation, deletion of *rebR* from the WT strain did not alter the phenotypic expression of stem nodules, but abolished the Fix<sup>-</sup> phenotype of nodules harboring the  $\Delta praR$  mutant so that the  $\Delta praR \Delta rebR$  mutant produced the Fix<sup>+</sup> phenotype (Fig. 4A). R bodies were not

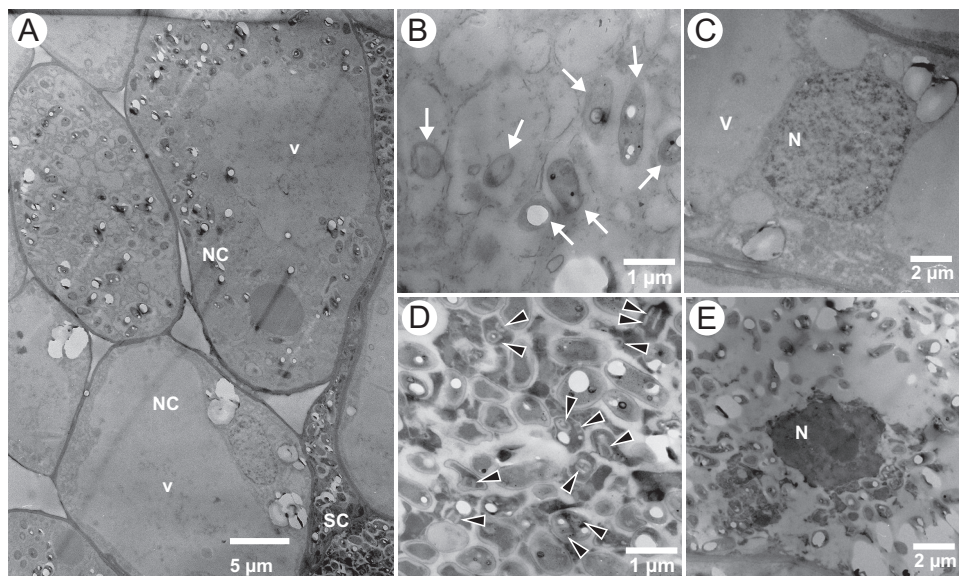


**FIG 3** TEM observations of stem nodules harboring the  $\Delta praR$  mutant at 7 dpi. (A) Normally shaped host cells (NC) with expanding vacuoles (v) and shrunken host cells (SC). (B and C) Bacterial cells (B) and host nuclei (C) in normally shaped cells. (D and E) Bacterial cells (D) and nuclei (E) in shrunken host cells. Arrows in panel B indicate bacterial cells, and arrowheads in panel D indicate R bodies. v, vacuole; N, nuclei.

observed in the  $\Delta praR \Delta rebR$  cells in the stem nodules (Fig. 4B). However, in symbiotic stem nodules, *reb* operon expression in the  $\Delta praR$  mutant was more than 10-fold higher than that in the  $\Delta praR \Delta rebR$  mutant and was about 2 orders of magnitude higher than that in the WT strain, whereas levels of *reb* operon expression were similar in the WT

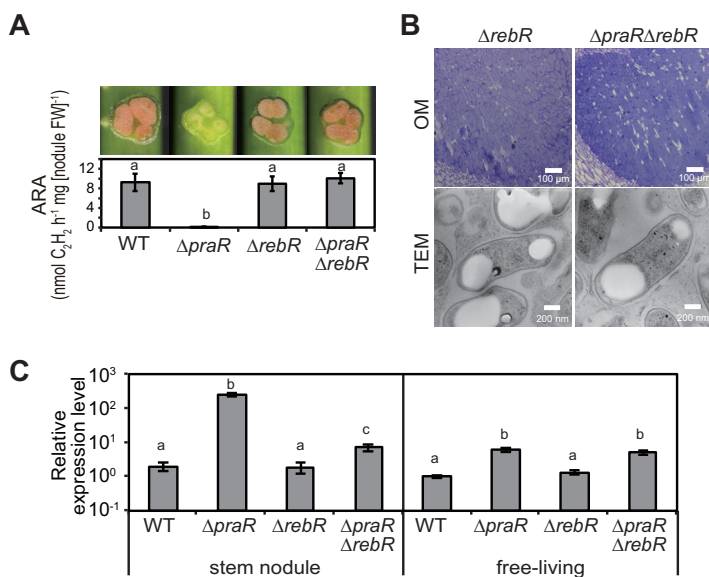


**FIG 4** Phenotypes of *praR* and/or *rebR* mutants. *S. rostrata* plants were inoculated with the WT or  $\Delta praR$ ,  $\Delta rebR$ , or  $\Delta praR \Delta rebR$  mutant strains and grown at 30°C, and stem nodules were analyzed at 14 dpi. (A) Hand-cut images (upper) and ARAs (lower) of stem nodules. Values are presented as means  $\pm$  standard deviations from five separate plants. Different letters indicate significant differences ( $P < 0.05$ , Tukey-Kramer). (B) OM observations of infected host cells in stem nodules and TEM observations of harbored bacterial cells. (C) Relative expression levels of the *reb* operon in stem nodules and free-living cultures. Total RNAs were isolated from bacteria residing in stem nodules and from bacterial cultures after growth to an OD<sub>600</sub> of approximately 1.0 at 38°C. Expression levels of the *reb* operon were estimated using quantitative RT-PCR and were normalized to 16S rRNA. Data are presented as means  $\pm$  standard deviations of three replicate cultures and plants and are expressed relative to mRNA levels in free-living WT cultures. Statistical analyses were carried out for stem nodules and free-living cultures, respectively. Different letters indicate significant differences ( $P < 0.05$ ; Tukey-Kramer).

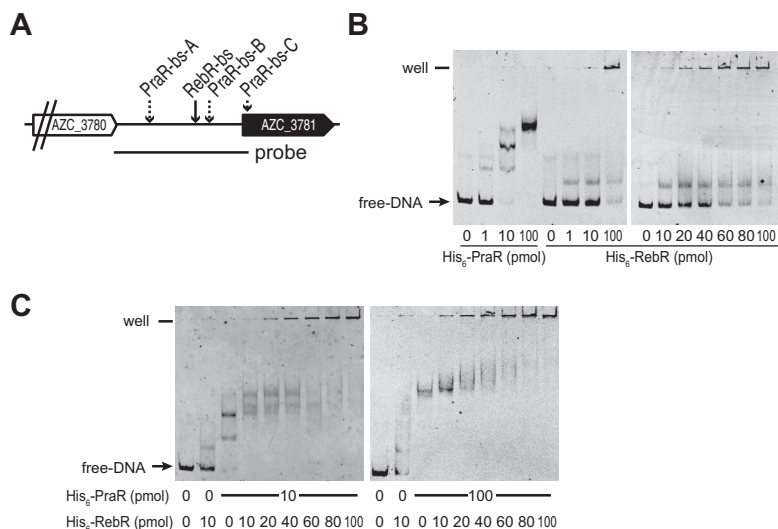


**FIG 5** *In vitro* binding activities of His<sub>6</sub>-PraR and His<sub>6</sub>-RebR to the *reb* promoter. (A) The region of the FITC-labeled dsDNA probe used in EMSA analyses. (B) EMSA analysis of dsDNA probes with increasing levels of purified His<sub>6</sub>-PraR or His<sub>6</sub>-RebR. (C) EMSA analysis of dsDNA probes with both His<sub>6</sub>-PraR and His<sub>6</sub>-RebR.

and  $\Delta rebR$  mutant strains (Fig. 4C). In contrast, in the free-living state, *reb* operon expression in the  $\Delta praR$  mutant was similar to that in the  $\Delta praR \Delta rebR$  mutant. These results indicate that although PraR predominantly represses the expression of the *reb* operon, RebR acts an activator of the operon under conditions of symbiosis.

**PraR and RebR directly control the *reb* operon.** Following a systematic evolution of ligands by exponential enrichment (SELEX) analysis, Frederix et al. (18) proposed that PraR of *R. leguminosarum* binds the consensus palindrome CAAC-N5-GTTG. In the present SELEX analysis using N-terminally His<sub>6</sub>-tagged PraR (His<sub>6</sub>-PraR) from *A. caulinodans*, the consensus PraR sequence of *A. caulinodans* was also CAAC-N5-GTTG (see Fig. S5A in the supplemental material). However, no sequence on the promoter region of the *reb* operon (*reb* promoter) matched this consensus sequence perfectly or with a base substitution, whereas four sequences matched with two or three substitutions, and these were examined as candidates for PraR binding sites. Subsequent electrophoretic mobility shift assays (EMSAs) revealed that His<sub>6</sub>-PraR binds strongly to a sequence designated PraR-bs-A and weakly to the sequences of PraR-bs-B and -C (Fig. S5B and C). Meanwhile, SELEX analysis using N-terminally His<sub>6</sub>-tagged RebR (His<sub>6</sub>-RebR) revealed that RebR potentially binds to a consensus palindrome, GT(A/G)(A/C)C-N4-G(T/G)(T/C)AC (Fig. S5D). A sequence (designated RebR-bs) matching this consensus palindrome was present on the *reb* promoter, and the EMSA revealed that His<sub>6</sub>-RebR binds to this sequence (Fig. S5E). The positions of PraR-bs-A, -B, and -C and RebR-bs on the *reb* promoter are shown in Fig. 1.

To investigate whether PraR and RebR actually bind to the *reb* promoter, we carried out EMSAs using a double-stranded DNA (dsDNA) probe that covers the intergenic noncoding region upstream of the *reb* operon (*reb* promoter dsDNA probe) as shown in Fig. 5A. The molecular weight (MW) of the *reb* promoter dsDNA probe increased with the increasing quantity of His<sub>6</sub>-PraR, whereas addition of His<sub>6</sub>-RebR to the promoter probe increased not only the MW of the probe but also the amount of stacked probe in the wells of the gel in a concentration-dependent manner (Fig. 5B). Even in the presence of His<sub>6</sub>-PraR, the addition of His<sub>6</sub>-RebR to the promoter probe increased the MW of the probe (Fig. 5C), indicating that PraR does not interfere the binding of RebR to the RebR-bs.

To confirm the involvement of PraR and RebR in *reb* operon expression, the significance of the promoter sequences was assessed in stem nodules that were formed

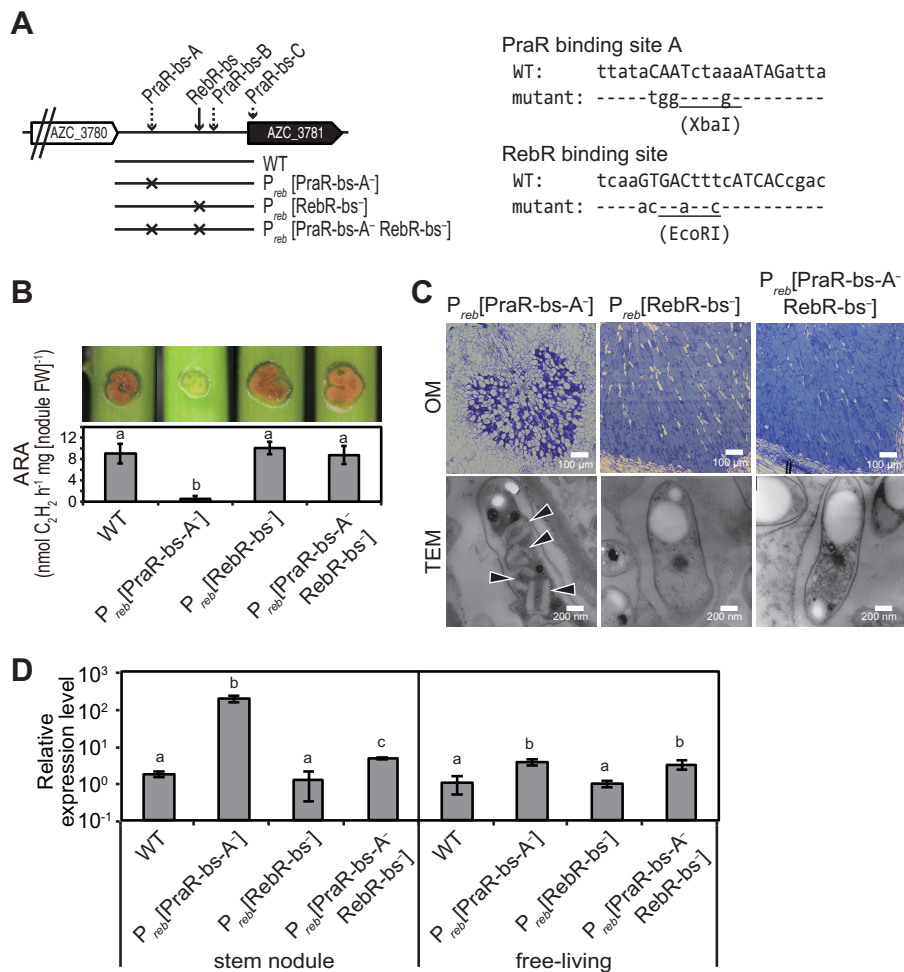


**FIG 6** Phenotypes of PraR-*bs*-A and/or RebR-*bs* mutants. (A) Mutants with base substitutions in PraR-*bs*-A [ $P_{reb}(\text{PraR-}bs\text{-}A^-)$  mutant], RebR-*bs* [ $P_{reb}(\text{RebR-}bs\text{-})$  mutant], or both genes [ $P_{reb}(\text{PraR-}bs\text{-}A^- \text{ RebR-}bs\text{-})$  double mutant] on the *reb* promoter. The sequences of the PraR binding site A and RebR binding site regions are shown in the right-hand side. The sequences corresponding to consensus palindromes are indicated in capital letters. Restriction endonuclease recognition sites (XbaI and EcoRI) were generated using the base substitutions. Mutants were inoculated into stems of *Sesbania* plants grown at 30°C, and stem nodules were analyzed at 14 dpi. (B) Hand-cut images (upper) and ARAs (lower) of the stem nodules formed by the indicated strains. Data are presented as means  $\pm$  standard deviations from five separate plants. Different letters indicate significant differences ( $P < 0.05$ , Tukey-Kramer). (C) OM observations of infected host cells in stem nodules and TEM observations of residing symbiotic bacterial cells. Arrowheads indicate R bodies. (D) Relative expression levels of the *reb* operon in bacteria from stem nodules and free-living cultures. Total bacterial RNA was isolated from bacteria that were grown in stem nodules and from free-living cultures grown in the defined medium at 38°C to an  $OD_{600}$  of approximately 1.0. Expression levels of the *reb* operon were estimated using quantitative RT-PCR, normalized to 16S rRNA levels, and expressed relative to corresponding mRNA levels in free-living WT cultures and are presented as means  $\pm$  standard deviations from three replicate cultures and plants. Statistical analyses were carried out for stem nodules and free-living cultures, respectively. Different letters indicate significant differences ( $P < 0.05$ , Tukey-Kramer).

after inoculation with mutants carrying base substitutions of  $P_{reb}(\text{PraR-}bs\text{-}A^-)$  and  $P_{reb}(\text{RebR-}bs\text{-})$  mutants and after inoculation with the  $P_{reb}(\text{PraR-}bs\text{-}A^- \text{ RebR-}bs\text{-})$  double mutant (Fig. 6A). Stem nodules harboring the  $P_{reb}(\text{PraR-}bs\text{-}A^-)$  mutant had the Fix<sup>-</sup> phenotype, whereas those harboring the  $P_{reb}(\text{PraR-}bs\text{-}A^- \text{ RebR-}bs\text{-})$  double mutant had restored nitrogen-fixing activity (Fig. 6B). Accordingly, R bodies were observed in  $P_{reb}(\text{PraR-}bs\text{-}A^-)$  mutants but not in  $P_{reb}(\text{PraR-}bs\text{-}A^- \text{ RebR-}bs\text{-})$  double mutants in stem nodules (Fig. 6C). In further experiments, expression levels of the *reb* operon in  $P_{reb}(\text{PraR-}bs\text{-}A^-)$  mutants and  $P_{reb}(\text{PraR-}bs\text{-}A^- \text{ RebR-}bs\text{-})$  double mutants were about 2 orders of magnitude and several times higher than those in the WT strain, respectively, whereas *reb* operon expression levels in the  $P_{reb}(\text{RebR-}bs\text{-})$  mutant were similar to

those in the WT strain (Fig. 6D). The consistency of phenotypic expression between deletion mutants of *praR* and *rebR* ( $\Delta praR$ ,  $\Delta rebR$ , and  $\Delta praR \Delta rebR$  mutants in Fig. 4) and corresponding promoter sequence mutants strongly indicates that PraR and RebR directly control the expression of the *reb* operon.

**Identification of environmental factors that abolish *reb* repression by PraR.** In the experiments described above, symbiotic R-body production was observed in  $\Delta praR$  and  $P_{reb}$ (PraR-bs-A<sup>-</sup>) mutants but was not present in the WT strain under symbiotic or free-living conditions, suggesting that R-body production is subjected to environmental conditions. Thus, we investigated environmental factors that induce RebR-dependent activation of the *reb* operon in the  $\Delta praR$  mutant and then identified factors that attenuate PraR-dependent repression of the *reb* operon in WT cells grown under the identified favorable environmental conditions.

Initially, we constructed a *reb* operon-*lacZ* transcriptional fusion (*reb-lacZ*) on chromosomes of the WT and  $\Delta praR$  strains, namely *reb-lacZ* and *reb-lacZ*  $\Delta praR$  strains, respectively. During these manipulations, the *reb-lacZ*  $\Delta praR$  strain expressed  $\beta$ -galactosidase in the free-living state at room temperature (around 26°C) but not at 38°C, suggesting that activation by RebR is temperature dependent. Accordingly, when *reb-lacZ* and *reb-lacZ*  $\Delta praR$  strains were grown at various temperatures between 26 and 41°C,  $\beta$ -galactosidase activity was highly induced below 35°C in the *reb-lacZ*  $\Delta praR$  strain, but not in the *reb-lacZ* strain (Fig. 7A). Moreover, expression levels of the *reb* operon were about 30-fold higher at 26°C than at 38°C in the  $\Delta praR$  strain, whereas activation at 26°C was not observed in either the  $\Delta rebR$  or  $\Delta praR \Delta rebR$  mutant (Fig. 7B). Under free-living conditions, R bodies were observed in up to 10% of  $\Delta praR$  cells grown at 26°C, but not in those grown at 38°C (Fig. 7C). Similarly,  $\Delta praR$  cells in stem nodules (symbiotic state) failed to produce R bodies when plants were grown at 38°C, and *reb* operon expression was lower than that in  $\Delta praR$  cells under symbiotic conditions at 30°C (see Fig. S6 in the supplemental material). Taken together, these data indicate that activation of the *reb* operon by RebR is temperature dependent under both free-living and symbiotic conditions. However, binding of RebR to the *reb* promoter was not affected by temperature (see Fig. S7 in the supplemental material).

In subsequent experiments, the effects of host-derived tricarboxylic acid (TCA) cycle, nitrogen, and oxygen metabolites on *reb* expression were investigated in *reb-lacZ* and *reb-lacZ*  $\Delta praR$  strains. In the absence of *praR* (the *reb-lacZ*  $\Delta praR$  strain), all organic acids except for citrate promoted *reb* expression under nitrogen-sufficient conditions at either 21 or 3% oxygen (Fig. 8). However, even in the presence of *praR* (*reb-lacZ* strain), *reb* expression was induced in medium containing 2-oxoglutarate (2OG) with sufficient nitrogen sources (Fig. 8). Moreover, induction was increased with 2OG concentrations even in the presence of succinate as a carbon source (Fig. 9A), suggesting that 2OG induces *reb* irrespective of its metabolism as a carbon source, although these effects of 2OG were observed at 26°C but not at 38°C (Fig. 9B). In agreement, TEM observations showed that R bodies were produced in WT cells grown in the presence of 2OG at 26°C but not at 38°C (Fig. 9C). Taken with the absence of a response to 2OG in  $\Delta rebR$  mutant cells (Fig. 9D), these observations indicate that *rebR* is essential for 2OG-mediated induction of the *reb* operon. Moreover, the  $\Delta praR$  mutants did not respond to 2OG, further suggesting that 2OG derepresses the *reb* operon by attenuating PraR-dependent repression. Western blotting of an *rgs-his<sub>6</sub>-praR* transformant (19) showed that expression levels of RGS-His<sub>6</sub>-PraR protein were not affected by 2OG (Fig. 9E). However, binding of PraR to the *reb* promoter dsDNA probe decreased with increasing 2OG concentration, whereas RebR binding was impervious to 2OG (Fig. 9F; Fig. S7). These observations strongly suggest that 2OG derepresses the *reb* operon directly by concentration-dependently inhibiting PraR binding to the *reb* promoter.

## DISCUSSION

In this study, we demonstrated that *reb*-driven pathogenicity is associated with R-body production by *A. caulinodans* and suggest that R-body production is a widespread trait among bacterial pathogens that carry *reb* operons. Although the *reb*

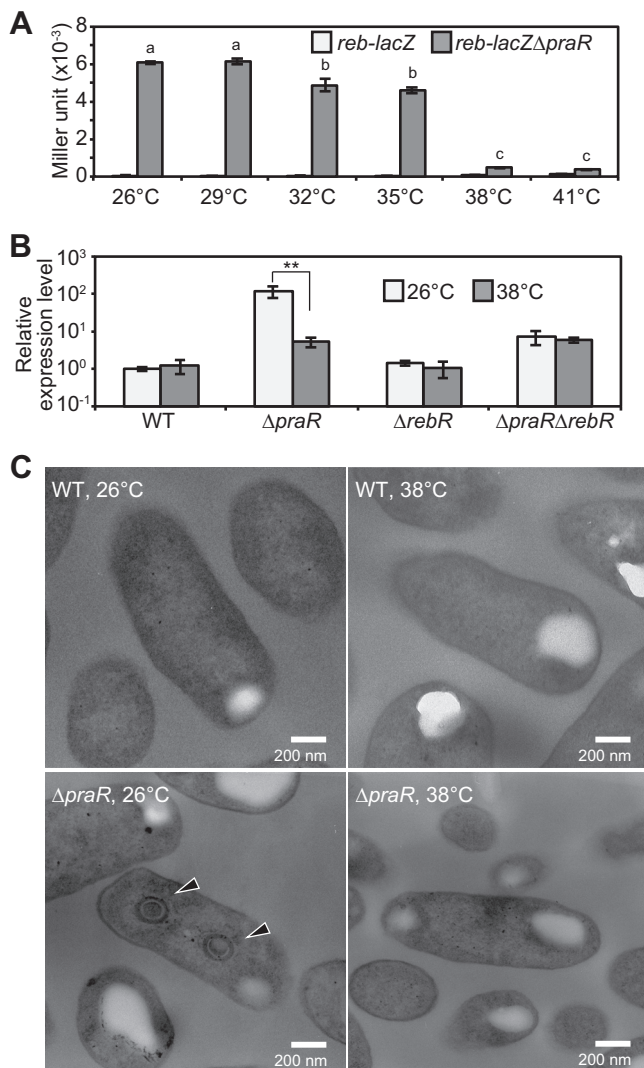


**FIG 7** Effects of temperature on the expression of the *reb* operon and R-body formation in free-living *A. caulinodans* cells. (A)  $\beta$ -Galactosidase activities of *reb-lacZ* and *reb-lacZ*  $\Delta$ *praR* strains. Bacterial cells were grown in the defined medium at the indicated temperatures to an OD<sub>600</sub> of approximately 1.0, and  $\beta$ -galactosidase activities were measured. Data are presented as means  $\pm$  standard deviations from three replicate cultures. Statistical analysis was carried out for the *reb-lacZ*  $\Delta$ *praR* strain. Different letters indicate significant differences ( $P < 0.05$ , Tukey-Kramer). (B) Quantitative RT-PCR analysis of the *reb* operon in the WT and  $\Delta$ *praR*,  $\Delta$ *rebR*, and  $\Delta$ *praR*  $\Delta$ *rebR* mutant strains grown at 26 and 38°C. Data are expressed relative to those from the WT strain grown at 26°C and are presented as means  $\pm$  standard deviations from three replicate cultures. Statistical analyses were carried out for each strain, respectively. Asterisks indicate significant difference (\*\*,  $P < 0.01$ , Student's *t* test). (C) TEM observations of free-living WT and  $\Delta$ *praR* strains. Bacterial cells were collected from the same cultures that were used for the quantitative RT-PCR analyses described in panel B. Arrowheads indicate R bodies.

operon is predominantly repressed by PraR, we identified biological and environmental factors that derepress *reb* gene expression and thus R-body production under free-living conditions.

R bodies are rolled up at neutral pH, but reportedly unroll to form needle-shaped structures at low pH (10). Recombinant R bodies from *Escherichia coli* act as pistons that puncture spheroplasts of *E. coli* at low pH (20). In paramecia, the role of R bodies in the killer trait follows release of R-body-containing bacteria from killer paramecia and ingestion by sensitive paramecia. Subsequently, internalized bacteria enter acidified food vacuoles, and R bodies are unrolled and penetrate the phagosomal membrane to deliver lethal toxins to the cytoplasm (9, 21). This scenario may also be applicable to interactions of *A. caulinodans* and *S. rostrata*, in which the peribacteroid space (mi-

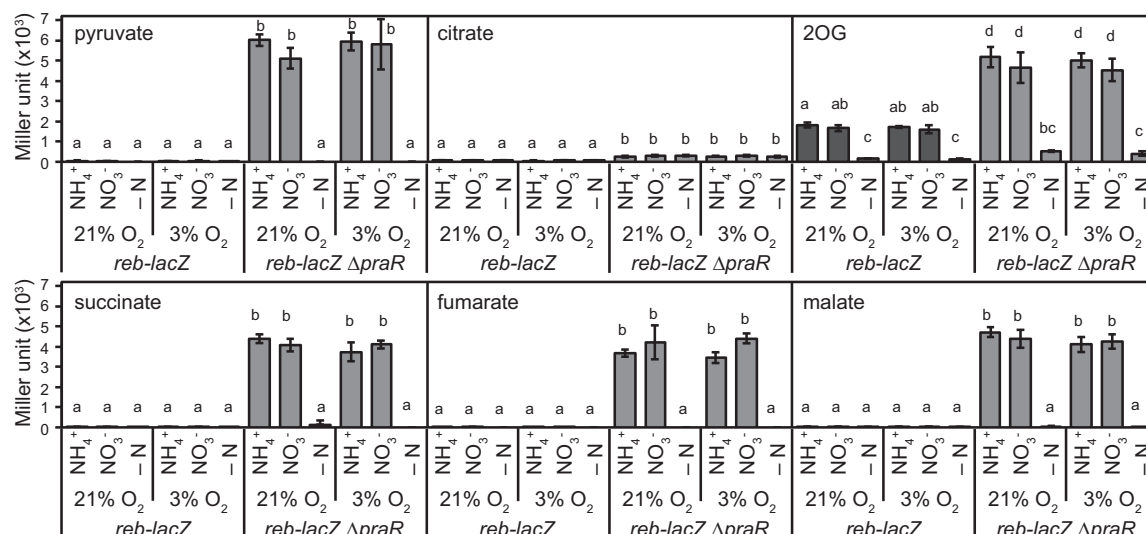


**FIG 8** Effects of carbon and nitrogen sources and oxygen concentrations on the expression of the *reb* operon under free-living conditions. Mutant *reb-lacZ* and *reb-lacZ ΔpraR* strains were grown in medium containing 50 mM pyruvate, citrate, 2-oxoglutarate (2OG), succinate, fumarate, or malate as carbon sources and 10 mM NH<sub>4</sub><sup>+</sup> or NO<sub>3</sub><sup>-</sup> as nitrogen sources or without a nitrogen source (-N) under aerobic (21% O<sub>2</sub>) or microaerobic (3% O<sub>2</sub>) conditions. Initial OD<sub>600</sub> values of cultures were adjusted to 0.02 for pyruvate, succinate, fumarate, and malate media with NH<sub>4</sub><sup>+</sup> or NO<sub>3</sub><sup>-</sup> supplementation, 0.1 for supplementation with 2OG and NH<sub>4</sub><sup>+</sup> or NO<sub>3</sub><sup>-</sup>, and 0.2 for supplementation with citrate medium and NH<sub>4</sub><sup>+</sup> or NO<sub>3</sub><sup>-</sup> or nitrogen-deficient media. After incubation at 26°C for 24 h, β-galactosidase activities were measured. Data are presented as means ± standard deviations from three replicate cultures. Different letters indicate significant differences ( $P < 0.05$ , Tukey-Kramer).

croenvironment surrounding bacteroids) is progressively acidified during nodule morphogenesis (22), likely triggering the conformational change of R bodies into the needle-shaped structure that penetrates membranes.

The present series of mutant analyses showed that essential genes for R-body formation in *A. caulinodans* include both *reb*-homologous and non-*reb*-homologous genes. Although the roles of the proteins encoded by the *reb*-homologous genes remain poorly understood, they are likely to be components of R bodies (5). Among non-*reb*-homologous genes, AZC\_3784 was found in the *reb* operon and was also essential to R-body formation. In *C. taeniospiralis*, RebC is encoded by a non-*reb*-homologous gene that may be involved in the assembly of R bodies (5). Similarly, the AZC\_3784 protein is not a component of R bodies but is likely involved in their assembly, although it may lack homology to *rebC* from *C. taeniospiralis*. Taken together, these observations warrant further compositional analyses of R bodies and investigations of the molecular mechanisms of R-body formation.

R bodies were frequently produced by *ΔpraR* mutants in the symbiotic state, but were observed in fewer than 10% of free-living cells, even at the optimum temperature (26°C) for *reb* operon expression. These results suggest that R-body formation is more strongly regulated (suppressed) in the free-living state—probably at the translation level or at the R-body assembly level—and that *A. caulinodan* R bodies play more important roles in the symbiotic state.

Although R-body formation was not observed in WT bacterial cells in the symbiotic state, the present environmental factors that derepress the *praR* regulatory system have significant implications for the understanding of *reb* operon evolution during microsymbiosis of *A. caulinodan* with *S. rostrata*. It is widely accepted that virulence genes are regulated by temperature in many pathogenic bacteria and are upregulated in mammalian bacterial pathogens at around host body temperature (37°C) (23, 24). In contrast, most plant-pathogenic bacteria express virulence genes at ambient temperatures that are generally lower than their optimal growth temperatures (25). For example, *Agrobacterium tumefaciens* mediates the formation of crown galls at temperatures below 32°C, and the VirA/VirG two-component system regulates the expression of virulence genes according to temperature (26, 27). In agreement, the *reb* operon was

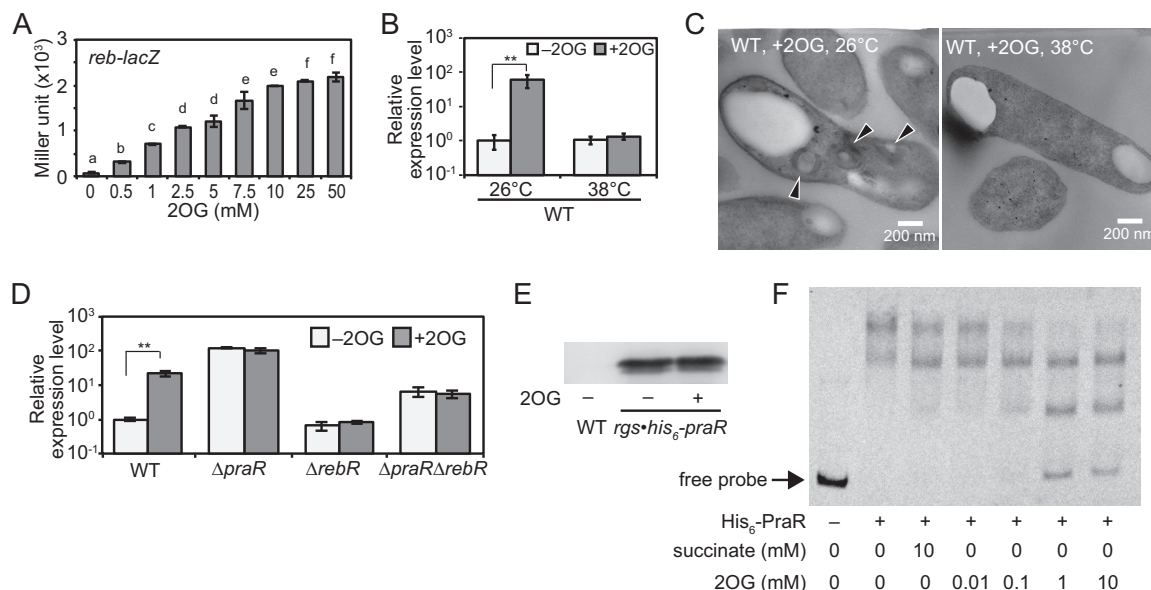


**FIG 9** Effects of 2OG on the expression of the *reb* operon and R-body formation in bacteria under free-living conditions. (A)  $\beta$ -Galactosidase activities of the *reb-lacZ* strain in the presence of various 2OG concentrations. The *reb-lacZ* strain was grown in medium with the indicated concentrations of 2OG (0 to 50 mM) at 26°C for 24 h to an  $OD_{600}$  of approximately 1.0. Data are presented as means  $\pm$  standard deviations from three replicate cultures. Different letters indicate significant differences ( $P < 0.05$ , Tukey-Kramer). (B) Quantitative RT-PCR analysis to investigate the effects of 2OG and temperature on the *reb* operon expression in the WT strain. Cultures of the WT strain were supplemented with 10 mM 2OG (+2OG) or no 2OG (-2OG) and were grown at 26 or 38°C. The data are expressed relative to those from the cultures under -2OG conditions at 26°C and are presented means  $\pm$  standard deviations from three replicate cultures. Asterisks indicate significant difference (\*\*,  $P < 0.01$ , Student's *t* test). (C) TEM observations of the WT cells cultured with 2OG at 26 and 38°C. Bacterial cells were collected from the cultures that were used for the quantitative RT-PCR conducted in panel B. Arrowheads indicate R bodies. (D) Quantitative RT-PCR analysis of the *reb* operon in the WT,  $\Delta praR$ ,  $\Delta rebR$ , and  $\Delta praR \Delta rebR$  strains. These strains were grown under +2OG or -2OG conditions at 26°C. The data are expressed relative to corresponding values in the WT strain under -2OG conditions at 26°C and are presented as means  $\pm$  standard deviations from three replicate cultures. Asterisks indicate significant difference (\*\*,  $P < 0.01$ , Student's *t* test). (E) Western blotting with an anti-His<sub>6</sub> antibody to investigate the effects of 2OG on RGS-His<sub>6</sub>-PraR expression. Whole-cell lysates from the *rgs-his<sub>6</sub>-praR* strain grown under +2OG or -2OG conditions and from the WT strain grown under -2OG conditions were electrophoresed. (F) EMSA analysis to investigate the effects of 2OG on binding activities of His<sub>6</sub>-PraR to the *reb* promoter. FITC-labeled dsDNA probe corresponding to the *reb* promoter was incubated with the purified His<sub>6</sub>-PraR in the presence of 2OG (0.01 to 10 mM) or succinate (10 mM).

expressed in the  $\Delta praR$  mutant of *A. caulinodans* at temperatures below 35°C and within the optimal range for the growth of the host plant (around 30°C). Moreover, because regulation by PraR was derepressed by 2OG in the present free-living WT cells at 26°C, the *reb* operon may also be induced during symbiosis in host nodules, wherein the 2OG is accumulated in the host plant cells, although we have not found the conditions under which 2OG actually accumulates in the host plant cells. Plant 2OG levels reflect cellular C/N status and may play a signaling role in the coordination of C and N metabolism (28). Alterations in the activities of nitrogen fixation by bacteria and ammonia assimilation by plant cells may lead to 2OG accumulation in host cells. To elucidate the roles of *reb* operon in the symbiotic state, we need to conduct more investigations to estimate the conditions wherein 2OG is accumulated in the host plant cells.

Although PraR homologues are widespread among *Alphaproteobacteria* (8), the roles of PraR have not been well characterized. In particular, the *praR* homologue *phrR* was originally identified in the acid-tolerant rhizobium *Sinorhizobium medicae* WSM419 as a gene that is induced at low pH (29). However, *praR* expression is not pH sensitive in *A. caulinodans* and *Rhizobium leguminosarum* (8, 18). Moreover, *R. leguminosarum* PraR directly represses the expression of the quorum-sensing genes *rhlR* and *rhlR* and the biofilm formation genes *rapA2*, *rapB*, and *rapC* (18, 30), whereas the homologous genes in *A. caulinodans* are not controlled by PraR (8). Hence, although PraR homologues are widely distributed, the roles of PraR have diversified during the evolution of *Alphaproteobacteria*. The ubiquity of chemical and environmental factors that regulate

*praR* expression in the *Alphaproteobacteria*, such as the effects of *A. caulinodans* factors, also requires investigation in the context of the evolution of *praR* regulatory systems.

RebR belongs to a novel subfamily of the Crp-Fnr superfamily, and all Crp-Fnr members carry putative DNA-binding helix-turn-helix domains on their C terminus and ligand-binding domains on their N terminus (17). Various intracellular and exogenous signals activate Crp-Fnr members via their ligand-binding domains, including 2OG and temperature (17). In *A. caulinodans*, however, binding activity of RebR to the *reb* operon was not affected by 2OG and temperature, indicating that in addition to 2OG and temperature, as yet unidentified factors are involved in the activation of *reb* operon expression via RebR.

Herein, we demonstrated the roles of R bodies in the pathogenicity of bacteria that harbor the *reb* operon, although the ensuing roles in nodule symbiosis and the related evolutionary implications remain uncharacterized. Because bacterial genomes are plastic, endosymbionts may become pathogenic after acquiring the *reb* operon if they do not suppress its expression. Although we did not determine whether R bodies threaten biodiversity or ecosystems, this possibility may require solutions in the future. Unlike obligate endosymbionts of paramecia, *A. caulinodans* can be cultured *in vitro* and genetic manipulation techniques have been established in this bacterium, warranting further use of *A. caulinodans* as a model for studies of R-body/*reb* genes.

## MATERIALS AND METHODS

**Bacterial strains and culture conditions.** The bacterial strains used in this study are listed in Table S1 in the supplemental material. *A. caulinodans* strains were grown in tryptone-yeast extract (TY) medium (31) or in basal defined (BD) medium containing 50 mM disodium succinate, 10 mM NH<sub>4</sub>Cl, 10 mM potassium phosphate (pH 7.0), 100 mg liter<sup>-1</sup> MgSO<sub>4</sub>·7H<sub>2</sub>O, 50 mg liter<sup>-1</sup> NaCl, 40 mg liter<sup>-1</sup> CaCl<sub>2</sub>·2H<sub>2</sub>O, 5.4 mg liter<sup>-1</sup> FeCl<sub>3</sub>·6H<sub>2</sub>O, 5 mg liter<sup>-1</sup> Na<sub>2</sub>MoO<sub>4</sub>·2H<sub>2</sub>O, 2 mg liter<sup>-1</sup> biotin, 4 mg liter<sup>-1</sup> nicotinic acid, and 4 mg liter<sup>-1</sup> pantothenic acid. To vary the carbon and nitrogen contents of BD medium, disodium succinate was replaced with sodium pyruvate, trisodium citrate, disodium 2-oxoglutarate, disodium fumarate, or disodium L-malate, and NH<sub>4</sub>Cl was replaced with KNO<sub>3</sub> or omitted. In some experiments, BD medium was further supplemented with disodium 2OG. To grow *A. caulinodans* strains under aerobic conditions, test tubes containing medium were sealed with butyl rubber septums, and the contained air was replaced with N<sub>2</sub> gas with 3% O<sub>2</sub>. Before inoculation into BD medium, bacterial cells were cultured overnight in TY medium and were washed twice in 10 mM potassium phosphate buffer (pH 7.0). Unless otherwise noted, initial optical density at 600 nm (OD<sub>600</sub>) values of cultures were adjusted to 0.1 or 0.02 for growth at 26 or 38°C, respectively, and OD<sub>600</sub> values were approximately 1.0 after 24 h of incubation.

**Construction of deletion and substitution mutants.** The plasmids and primers used for strain construction are listed in Tables S1 and S2 in the supplemental material, respectively.

To construct *A. caulinodans* deletion mutants of AZC\_3784, AZC\_3785, AZC\_3787, and *rebR* genes, two DNA fragments containing upstream and downstream regions of each gene were amplified from the WT genomic DNA by PCR using appropriate primer pairs and were then directionally cloned into a suicide vector, pK18*mobsacB* (32), using the In-Fusion cloning kit (Clontech, Mountain View, CA). The linearization of pK18*mobsacB* was performed by inverse PCR using the PrimeSTAR Max (TaKaRa-Bio, Shiga, Japan) with primer pair Tp73-Tp74. The resulting plasmids were conjugated into the WT or  $\Delta$ *praR* (8) strains via *E. coli* S17-1( $\lambda$ pir) (33), and gene deletions were introduced by allelic exchange.

To construct deletion mutants of the *reb*<sub>AZC1</sub>, *reb*<sub>AZC2</sub>, *reb*<sub>AZC3</sub>, and *reb*<sub>AZC4</sub> genes, a series of plasmids were constructed as follows. DNA fragments containing the WT AZC\_3781-7 region with its upstream and downstream regions were amplified by PCR and cloned into the linearized pK18*mobsacB*. Genes on plasmids containing the WT region were deleted by inverse PCR using the PrimeSTAR Mutagenesis Basal kit (TaKaRa-Bio). To introduce double deletions, second inverse PCRs were conducted using plasmids harboring single mutations. Constructed plasmids were conjugated into the  $\Delta$ *praR*  $\Delta$ AZC\_3781-7 mutant, and deletion mutants were obtained after allelic exchange.

To construct mutants with base substitutions in PraR-bs-A and/or RebR-bs, a series of plasmids were constructed as follows. A DNA fragment containing the WT *reb* promoter region was amplified by PCR and cloned into the linearized pK18*mobsacB*. An XbaI site was generated within the PraR-bs-A on the plasmid containing the *reb* operon by inverse PCR using the PrimeSTAR Mutagenesis Basal kit. Similarly, an EcoRI site was generated within the RebR-bs on the plasmid containing the *reb* promoter. The resulting plasmids were conjugated into the WT strain, and mutants were obtained after allelic exchange.

To construct strains that express the *reb-lacZ* fusion gene, two fragments containing *rebR* and AZC\_3789 and a *lacZ* fragment were amplified by PCR from the WT genomic DNA and the plasmid pTA-MTL (34), respectively. Fragments were then cloned into the linearized pK18*mobsacB* in the direction of the *rebR*, *lacZ*, and AZC\_3789 fragments using the In-Fusion cloning kit. The plasmid containing *reb-lacZ* was conjugated into the WT and  $\Delta$ *praR* strains, and strains with *lacZ* at the position immediately downstream of the *rebR* open reading frame (ORF) were obtained after allelic exchange.

**Plant growth and bacterial inoculation for nodule formation.** *S. rostrata* stems were inoculated with *A. caulinodans* strains as described previously (19) and were then grown at 30 or 38°C under a 24-h light regimen. Acetylene reduction activities (ARAs) of stem nodules were assayed as described previously (19).

**Optical microscopy observation.** Stem nodules were longitudinally cut into three pieces. The middle pieces of each sample were chemically fixed with 4% paraformaldehyde and 2% glutaraldehyde, dehydrated through a graded ethanol series, and then embedded in Technovit 7100 (Heraeus Kulzer). The embedded samples were sliced into 5- $\mu$ m sections, stained with 0.05% toluidine blue O, and then observed using a bright-field microscope (DMLB; Leica).

**TEM observation.** Bacterial cells were collected from culture media by centrifugation. Stem nodules were cut into small pieces. These samples were chemically fixed as described above, postfixed with 2% OsO<sub>4</sub>, dehydrated through a graded ethanol series, and finally embedded in Spurr low-viscosity embedding medium (Polysciences, Warrington, PA). Embedded samples were then sliced into ultrathin (about 70-nm) sections, stained with uranyl acetate followed by lead citrate, and examined using a JEM-1010 electron microscope (JEOL, Tokyo, Japan) at an accelerating voltage of 100 kV.

**$\beta$ -Galactosidase assay.**  $\beta$ -Galactosidase activity was measured according to a previously reported method (35) with some modifications as follows. Fifty microliters of bacterial cultures was mixed with 450  $\mu$ l of Z buffer (60 mM Na<sub>2</sub>HPO<sub>4</sub>, 40 mM NaH<sub>2</sub>PO<sub>4</sub>, 10 mM KCl, 1 mM MgSO<sub>4</sub>) supplied with 50 mM 2-mercaptoethanol and 0.001% sodium dodecyl sulfate (SDS) and 50  $\mu$ l of chloroform. The mixture was vortexed for 30 s, and 50  $\mu$ l of *o*-nitrophenyl- $\beta$ -D-galactoside (ONPG [4 mg ml<sup>-1</sup> in Z buffer]) was added. After incubation at 25°C, reactions were stopped by adding 250  $\mu$ l of 1 M Na<sub>2</sub>CO<sub>3</sub>. Mixtures were centrifuged, and 200  $\mu$ l of the supernatants was transferred to 96-well clear plates. Subsequently, 200  $\mu$ l of the bacterial cultures was transferred to 96-well clear plates. The absorbance of the supernatant at 415 and 540 nm and optical density at 595 nm (OD<sub>595</sub>) of the cultures were measured using a microplate reader (680 XR; Bio-Rad, Hercules, CA).

**Total RNA extraction and quantitative RT-PCR.** Total RNA was isolated from bacterial cultures and stem nodules, and cDNA was synthesized according to previously described methods (19). Quantitative PCR was performed with a LightCycler system (Roche, Basel, Switzerland) using the QuantiTect SYBR green PCR kit (Qiagen, Hilden, Germany) with primer pairs Acp326-Acp714 for the *reb* operon and Tp35-Tp36 for 16S rRNA. Standard curves were generated using genomic DNA that was isolated from the WT strain using the NucleoSpin tissue kits (Macherey-Nagel, Düren, Germany). To determine expression levels of the *reb* operon, copy numbers of *reb* operon transcripts were normalized to those of 16S rRNA.

**Purification of His<sub>6</sub>-tagged PraR and RebR.** The *praR* ORF was amplified by PCR from the WT genomic DNA using primer pair Acp375-Acp161 and was then cloned into BamHI and XbaI restriction sites of the pCold I vector (TaKaRa-Bio, Shiga, Japan). The resulting plasmid was designated pTAC99. The *rebR* ORF was amplified by PCR from WT genomic DNA using primer pair Acp669-Acp670 and cloned into pCold I using the In-Fusion cloning kit (Clontech, Mountain View, CA). The linearization of pCold I was performed by inverse PCR using the PrimeSTAR Max (TaKaRa-Bio) with primer pair Tp78-Tp79. The resulting plasmid was designated pTAC133. pTAC99 and pTAC133 were transformed into *E. coli* BLR(DE3) (Novagen, Darmstadt, Germany). Subsequently, His<sub>6</sub>-PraR and His<sub>6</sub>-RebR were extracted and purified using Ni<sup>2+</sup>-charged magnetic beads (His Mag Sepharose Ni; GE Healthcare, Little Chalfont, United Kingdom). Eluted proteins were then concentrated using Vivaspin 500 kits (molecular weight cutoff [MWCO] of 5,000; Sartorius, Göttingen, Germany) and were mixed with 5 volumes of 1.2 $\times$  storage buffer (24 mM Tris-HCl [pH 8.0], 120 mM NaCl, 1.2 mM dithiothreitol [DTT], 60% glycerol).

**EMSA of the *reb* promoter.** Fluorescein isothiocyanate (FITC)-labeled dsDNA probes corresponding to the *reb* promoter region were prepared as follows. Initially, the *reb* promoter region was amplified by PCR using primer pair Acp646-Acp702 and genomic DNA from WT or derivative strains. Acp702 has an M13 reverse sequence at the 5' end. PCR products from each strain were purified using the MinElute PCR purification kit (Qiagen) and were used as the templates for the second round of PCR using primer pair Acp646-M13R\_FITC. Finally, FITC-labeled PCR products were purified. EMSAs were then performed by incubating 1-pmol aliquots of FITC-labeled dsDNA probes with various amounts of His<sub>6</sub>-PraR and/or His<sub>6</sub>-RebR in 20  $\mu$ l of EMSA buffer [20 mM Tris-HCl (pH 8.0), 1 mM EDTA, 60 mM NaCl, 5 mM MgCl<sub>2</sub>, 1 mM DTT, 10 ng  $\mu$ l<sup>-1</sup> poly(dI-dC), 4% glycerol, 0.05% Tween 20] for 30 min at 26°C. Binding reaction mixtures were then electrophoresed in 4% native polyacrylamide gels containing 2.5% glycerol in 0.5 $\times$  Tris-borate-EDTA (TBE) buffer, and FITC-labeled DNAs were detected using the LAS3000 system (Fuji Film, Tokyo, Japan).

**Western blotting analyses of RGS-His<sub>6</sub>-PraR.** Bacterial cells were collected from cultures by centrifugation, sonicated in phosphate-buffered saline (150 mM NaCl, 10 mM Na<sub>2</sub>HPO<sub>4</sub>, 20 mM NaH<sub>2</sub>PO<sub>4</sub> [pH 7.4]), and then fractionated by SDS-PAGE using 14% polyacrylamide gels. Fractionated proteins were electroblotted onto polyvinylidene difluoride (PVDF) membranes, incubated with mouse anti-His<sub>6</sub> antibody (Qiagen), and detected using horseradish peroxidase (HRP)-conjugated sheep anti-mouse antibodies (GE Healthcare) and the EzWestLumi Plus reagents (Atto, Tokyo, Japan).

## SUPPLEMENTAL MATERIAL

Supplemental material for this article may be found at <https://doi.org/10.1128/mBio.00715-17>.

**FIG S1**, PDF file, 0.2 MB.

**FIG S2**, PDF file, 0.2 MB.

**FIG S3**, PDF file, 1.2 MB.

**FIG S4**, PDF file, 1.1 MB.

**FIG S5**, PDF file, 0.3 MB.

**FIG S6**, PDF file, 0.4 MB.

**FIG S7**, PDF file, 0.2 MB.

**TABLE S1**, DOCX file, 0.1 MB.

**TABLE S2**, DOCX file, 0.1 MB.

## ACKNOWLEDGMENTS

We thank Fumiyasu Endo and Rio Yoguchi for technical assistance.

This work, including the efforts of Toshihiro Aono, was funded by the Japan Society for the Promotion of Science (JSPS) (25450081 and 16K07638).

## REFERENCES

- Anderson TF, Preer JR, Jr, Preer LB, Bray M. 1964. Studies on killing particles from *Paramecium*: the structure of refractile bodies from kappa particles. *J Microsc* 3:395–402.
- Pond FR, Gibson I, Lalucat J, Quackenbush RL. 1989. R-body-producing bacteria. *Microbiol Rev* 53:25–67.
- Sonneborn TM. 1938. Mating types in *Paramecium aureliae*: diverse conditions for mating in different stocks; occurrence, number and interrelations of the types. *Proc Am Philos Soc* 79:411–434.
- Dilts JA, Quackenbush RL. 1986. A mutation in the R body-coding sequence destroys expression of the killer trait in *P. tetraurelia*. *Science* 232:641–643. <https://doi.org/10.1126/science.3008334>.
- Heruth DP, Pond FR, Dilts JA, Quackenbush RL. 1994. Characterization of genetic determinants for R body synthesis and assembly in *Caedibacter taeniospiralis* 47 and 116. *J Bacteriol* 176:3559–3567. <https://doi.org/10.1128/jb.176.12.3559-3567.1994>.
- Jeblick J, Kusch J. 2005. Sequence, transcription activity, and evolutionary origin of the R-body coding plasmid pKAP298 from the intracellular parasitic bacterium *Caedibacter taeniospiralis*. *J Mol Evol* 60:164–173. <https://doi.org/10.1007/s00239-004-0002-2>.
- Sohn JH, Lee JH, Yi H, Chun J, Bae KS, Ahn TY, Kim SJ. 2004. *Kordia algicida* gen. nov., sp. nov., an algicidal bacterium isolated from red tide. *Int J Syst Evol Microbiol* 54:675–680. <https://doi.org/10.1099/ijs.0.02689-0>.
- Akiba N, Aono T, Toyazaki H, Sato S, Oyaizu H. 2010. *phrR*-like gene *praR* of *Azorhizobium caulinodans* ORS571 is essential for symbiosis with *Sesbania rostrata* and is involved in expression of *reb* genes. *Appl Environ Microbiol* 76:3475–3485. <https://doi.org/10.1128/AEM.00238-10>.
- Raymann K, Bobay L-M, Doak TG, Lynch M, Gribaldo S. 2013. A genomic survey of *Reb* homologs suggests widespread occurrence of R-bodies in proteobacteria. *G3* 3:505–516. <https://doi.org/10.1534/g3.112.005231>.
- Quackenbush RL, Burbach JA. 1983. Cloning and expression of DNA sequences associated with the killer trait of *Paramecium tetraurelia* stock 47. *Proc Natl Acad Sci U S A* 80:250–254. <https://doi.org/10.1073/pnas.80.1.250>.
- Beier CL, Horn M, Michel R, Schweikert M, Görtz HD, Wagner M. 2002. The genus *Caedibacter* comprises endosymbionts of *Paramecium* spp. related to the *Rickettsiales* (*Alphaproteobacteria*) and to *Francisella tularensis* (*Gammaproteobacteria*). *Appl Environ Microbiol* 68:6043–6050. <https://doi.org/10.1128/AEM.68.12.6043-6050.2002>.
- Lee KB, De Backer P, Aono T, Liu CT, Suzuki S, Suzuki T, Kaneko T, Yamada M, Tabata S, Kupfer DM, Najjar FZ, Wiley GB, Roe B, Binnewies TT, Ussery DW, D'Haese W, Herder JD, Gevers D, Vereecke D, Holsters M, Oyaizu H. 2008. The genome of the versatile nitrogen fixer *Azorhizobium caulinodans* ORS571. *BMC Genomics* 9:271. <https://doi.org/10.1186/1471-2164-9-271>.
- Dreyfus B, Garcia JL, Gillis M. 1988. Characterization of *Azorhizobium caulinodans* gen. nov., sp. nov., a stem-nodulating nitrogen-fixing bacterium isolated from *Sesbania rostrata*. *Int J Syst Bacteriol* 38:89–98. <https://doi.org/10.1099/00207713-38-1-89>.
- Dreyfus BL, Elmerich C, Dommergues YR. 1983. Free-living *Rhizobium* strain able to grow on N<sub>2</sub> as the sole nitrogen source. *Appl Environ Microbiol* 45:711–713.
- Dreyfus BL, Dommergues YR. 1981. Nitrogen-fixing nodules induced by *Rhizobium* on the stem of the tropical legume *Sesbania rostrata*. *FEMS Microbiol Lett* 10:313–317. <https://doi.org/10.1111/j.1574-6968.1981.tb06262.x>.
- Tsien HC, Dreyfus BL, Schmidt EL. 1983. Initial stages in the morphogenesis of nitrogen-fixing stem nodules of *Sesbania rostrata*. *J Bacteriol* 156:888–897.
- Körner H, Sofia HJ, Zumft WG. 2003. Phylogeny of the bacterial superfamily of Crp-Fnr transcription regulators: exploiting the metabolic spectrum by controlling alternative gene programs. *FEMS Microbiol Rev* 27:559–592. [https://doi.org/10.1016/S0168-6445\(03\)00066-4](https://doi.org/10.1016/S0168-6445(03)00066-4).
- Frederix M, Edwards A, McAnulla C, Downie JA. 2011. Co-ordination of quorum-sensing regulation in *Rhizobium leguminosarum* by induction of an anti-repressor. *Mol Microbiol* 81:994–1007. <https://doi.org/10.1111/j.1365-2958.2011.07738.x>.
- Nakajima A, Aono T, Tsukada S, Siarot L, Ogawa T, Oyaizu H. 2012. Lon protease of *Azorhizobium caulinodans* ORS571 is required for suppression of *reb* gene expression. *Appl Environ Microbiol* 78:6251–6261. <https://doi.org/10.1128/AEM.01039-12>.
- Polka JK, Silver PA. 2016. A tunable protein piston that breaks membranes to release encapsulated cargo. *Synth Biol* 5:303–311. <https://doi.org/10.1021/acssynbio.5b00237>.
- Jurand A, Rudman BM, Preer JR, Jr. 1971. Prelethal effects of killing action by stock 7 of *Paramecium aurelia*. *J Exp Zool* 177:365–387. <https://doi.org/10.1002/jez.1401770311>.
- Pierre O, Engler G, Hopkins J, Brau F, Boncompagni E, Hérouart D. 2013. Peribacteroid space acidification: a marker of mature bacteroid functioning in *Medicago truncatula* nodules. *Plant Cell Environ* 36:2059–2070. <https://doi.org/10.1111/pce.12116>.
- Konkel ME, Tilly K. 2000. Temperature-regulated expression of bacterial virulence genes. *Microbes Infect* 2:157–166. [https://doi.org/10.1016/S1286-4579\(00\)00272-0](https://doi.org/10.1016/S1286-4579(00)00272-0).
- Shapiro RS, Cowen LE. 2012. Thermal control of microbial development and virulence: molecular mechanisms of microbial temperature sensing. *mBio* 3:e00238-12. <https://doi.org/10.1128/mBio.00238-12>.
- Smirnova A, Li H, Weingart H, Aufhammer S, Burse A, Finis K, Schenk A, Ullrich MS. 2001. Thermoregulated expression of virulence factors in plant-associated bacteria. *Arch Microbiol* 176:393–399. <https://doi.org/10.1007/s002030100344>.
- Riker AJ. 1926. Studies on the influence of some environmental factors on the development of crown gall. *J Agric Res* 32:83–96.
- Jin S, Song YN, Deng WY, Gordon MP, Nester EW. 1993. The regulatory VirA protein of *Agrobacterium tumefaciens* does not function at elevated temperatures. *J Bacteriol* 175:6830–6835. <https://doi.org/10.1128/jb.175.21.6830-6835.1993>.
- Lancien M, Gadal P, Hodges M. 2000. Enzyme redundancy and the importance of 2-oxoglutarate in higher plant ammonium assimilation. *Plant Physiol* 123:817–824. <https://doi.org/10.1104/pp.123.3.817>.
- Reeve WG, Tiwari RP, Wong CM, Dilworth MJ, Glenn AR. 1998. The transcriptional regulator gene *phrR* in *Sinorhizobium meliloti* WSM419 is regulated by low pH and other stresses. *Microbiology* 144:3335–3342. <https://doi.org/10.1099/00221287-144-12-3335>.
- Frederix M, Edwards A, Swiderska A, Stanger A, Karunakaran R, Williams A, Abbruscato P, Sanchez-Contreras M, Poole PS, Downie JA. 2014. Mutation of *praR* in *Rhizobium leguminosarum* enhances root biofilms, improving nod-

- ulation competitiveness by increased expression of attachment proteins. *Mol Microbiol* 93:464–478. <https://doi.org/10.1111/mmi.12670>.
31. Beringer JE. 1974. R factor transfer in *Rhizobium leguminosarum*. *J Gen Microbiol* 84:188–198. <https://doi.org/10.1099/00221287-84-1-188>.
  32. Schäfer A, Tauch A, Jäger W, Kalinowski J, Thierbach G, Pühler A. 1994. Small mobilizable multi-purpose cloning vectors derived from the *Escherichia coli* plasmids pk18 and pk19: selection of defined deletions in the chromosome of *Corynebacterium glutamicum*. *Gene* 145:69–73. [https://doi.org/10.1016/0378-1119\(94\)90324-7](https://doi.org/10.1016/0378-1119(94)90324-7).
  33. Simon R, Priefer U, Pühler A. 1983. A broad host range mobilization system for *in vivo* genetic engineering: transposon mutagenesis in Gram negative bacteria. *Nat Biotechnol* 1:784–791. <https://doi.org/10.1038/nbt1183-784>.
  34. Iki T, Aono T, Oyaizu H. 2007. Evidence for functional differentiation of duplicated *nifH* genes in *Azorhizobium caulinodans*. *FEMS Microbiol Lett* 274:173–179. <https://doi.org/10.1111/j.1574-6968.2007.00823.x>.
  35. Miller JH. 1972. *Experiments in molecular genetics*. Cold Spring Harbor Laboratory, Cold Spring Harbor, NY.